

Doublon-Holon Binding Effects on Mott Transitions in Two-Dimensional Bose Hubbard Model

Hisatoshi Yokoyama^{a,*} Masao Ogata^b

^a*Department of Physics, Tohoku University, Sendai 980-8578, Japan.*

^b*Department of Physics, University of Tokyo, Bunkyo-ku, Tokyo 113-0033, Japan.*

Abstract

A mechanism of Mott transitions in a Bose Hubbard model on a square lattice is studied, using a variational Monte Carlo method. Besides an onsite correlation factor, we introduce a four-body doublon-holon factor into the trial state, which considerably improves the variational energy and can appropriately describe a superfluid-insulator transition. Its essence consists in binding (and unbinding) of a doublon to a holon in a finite short range, identical with the cases of fermions. The features of this transition are qualitatively different from those of Brinkman-Rice-type transitions.

Key words: Bose Hubbard model, Mott transition, doublon-holon binding factor, variational Monte Carlo method, square lattice

PACS: 67.40.-w, 05.30.Jp, 71.30.+h

1. Introduction: After early theoretical studies of Mott or superfluid-insulator transitions in interacting Bose systems [1], an experimental example has been realized using an ultracold dilute gas of bosonic atoms in an optical lattice [2]. The essence of this system is considered to be captured [3] by a Bose Hubbard model. This basic model has been studied with various methods; for square lattices, properties of T_c , superfluid density, etc. were studied, applying a quantum Monte Carlo method to small systems (mainly 6×6 square lattice) [4], and a ground-state phase diagram in a plane of chemical potential and interaction strength was obtained, using a strong-coupling expansion [5]. These studies estimated the critical interaction strength of Mott transitions at $U_c/t = 16.4 \pm 0.8$

* Corresponding author. TEL./fax: +81-22-795-6444
E-mail: yoko@cmpt.phys.tohoku.ac.jp (H. Yokoyama)

and 16.69, respectively, for the particle density of $n = 1$ ($n = N_e/N$ with N_e : particle number, N : site number) at $T = 0$. Thus, the existence of a Mott transition has been embodied, but the mechanism of the transition is still not clear.

Variational Monte Carlo approaches are very useful to understand the mechanism of the Mott transition, because one can directly and exactly treat wave functions. For the Bose Hubbard model, wave functions with only onsite correlation factors, which corresponds to the celebrated Gutzwiller wave function (GWF, Ψ_G) for fermions [6], were studied first [7]. In contrast to for fermions, GWF for bosons is solved analytically without additional mean-field-type approximations [8] for arbitrary dimensions, and yield a Brinkman-Rice-type (BR) transition [9] at $U = U_{BR}$. In BR transitions, all the lattice sites are occupied with exactly one particle and the hopping completely ceases in the insulating regime, namely, $\Psi_G \rightarrow \prod_{j=1}^N b_j^\dagger |0\rangle$ and $E = 0$ for $U > U_{BR}$. This result is caused by an oversimplified setup of the wave function, in which the effect of density fluctuation should be included. In this work, we introduce a doublon-holon binding correlation factor into the trial function, following previous studies for fermions. Thereby, we can describe a superfluid-insulator transition more appropriately.

2. Formulation: We consider a spinless Bose-Hubbard model on a square lattice,

$$H = -t \sum_{\langle ij \rangle} (b_i^\dagger b_j + b_j^\dagger b_i) + \frac{U}{2} \sum_j n_j(n_j - 1), \quad (1)$$

where b_j^\dagger is a creation operator of a boson at site j , $n_j = b_j^\dagger b_j$ and $t, U > 0$. Here, $\langle ij \rangle$ denotes a nearest-neighbor-site pair; the definition of t is a half of what was given in some literatures [4,7]. In this work, we restrict to $n \sim 1$, because we would like to consider the most simple case of Mott transitions. The cases of other commensurate densities ($n \geq 2$) must be essentially identical.

We study this model eq. (1) through a variation theory. As a trial wave function, we use a Jastrow type of $\Psi_Q = P_Q P_G \Phi$ (QWF), following previous studies for fermions [10,11]. Here, Φ is the ground state of noninteracting (completely coherent) bosons, namely $\Phi = 1$, P_G is an onsite

projector corresponding to the famous Gutzwiller factor for fermions [6]: $P_G(g) = g^D$, with $D = \sum_i n_i(n_i - 1)/2$. As we repeatedly showed [11,12], intersite correlation factors are indispensable for appropriate descriptions of interacting systems. In particular near half filling, a four-body doublon-holon correlation factor P_Q is crucial to explain the mechanism of Mott transitions [13,14,15]. For $S = 1/2$ fermions, P_Q is explicitly written as,

$$P_Q(\mu) = (1 - \mu)^{\tilde{Q}} \quad (2)$$

with $0 \leq \mu \leq 1$ and

$$\tilde{Q} = \sum_i \prod_\tau [d_i(1 - e_{i+\tau}) + e_i(1 - d_{i+\tau})], \quad (3)$$

where $d_i (= n_{i\uparrow}n_{i\downarrow})$ and $e_i [= (1 - n_{i\uparrow})(1 - n_{i\downarrow})]$ are the doublon and holon operators respectively, i runs over all the sites, and τ the four nearest-neighbor sites of the site i . When the variational parameter μ vanishes, Ψ_Q is reduced to the GWF, $\Psi_G = P_G \Phi$, in which doublons and holons can move independently. On the other hand, in the limit of $\mu \rightarrow 1$, a doublon becomes bound to a holon in nearest-neighbor sites. Consequently, plus (holons) and minus (doublons) charge carriers completely cancels, indicating a metal-insulator transition.

In this work, we extend eq. (2) to bosons, and include the correlation between diagonal (second-nearest)-neighbor sites:

$$P_Q(\mu, \mu') = (1 - \mu)^Q (1 - \mu')^{Q'}, \quad (4)$$

where the primes ($'$) denote the cases of diagonal neighbors. In eq. (4), Q has the same form as \tilde{Q} in eq. (3), but the doublon operator d_i is replaced by a multiplon operator m_i , which yields 1 (0) if the site i is multiply occupied (otherwise). Near Mott transitions, P_Q of eq. (4) is substantially a doublon-holon factor, because the probability density of multiplon with more than two bosons is almost zero for such large values of U/t .

To estimate expectation values accurately, we use a variational Monte Carlo method [16,17,18] of fixed particle numbers. First, we optimize the variational parameters, g , μ and μ' , simultaneously for each set of U/t , n and L , and then calculate physical quantities with the optimized parameters.

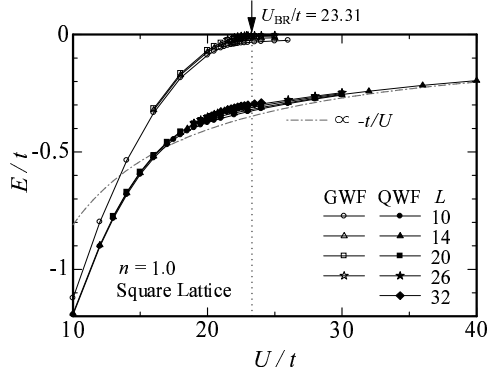


Fig. 1. Comparison of total energy per site between GWF and QWF as a function of U/t for several system sizes. The particle density is commensurate ($n = 1.0$). For GWF, a Brinkman-Rice-type transition occurs at $U = U_{BR}$. The dash-dotted line is a curve proportional to $-t/U$.

Through the optimization process, we average substantially several million samples, which reduces statistical errors in the total energy typically to the order of $10^{-4}t$. To check system-size dependence, particularly near phase transitions, we employ square lattices of $N = L \times L$ sites up to $N = 1024$ ($L = 32$) with the periodic-periodic boundary conditions.

3. Results: We start with comparison of the total energies E/t between GWF and QWF, which are shown in Fig. 1 for $n = 1$. As mentioned, in GWF [7], a BR transition occurs at $U_{BR}/t = 12 + 8\sqrt{2} = 23.31\dots$; for $U > U_{BR}$, each site is occupied by exactly one particle and hopping or density fluctuation completely ceases. Consequently, E/t vanishes in the insulating regime. On the side of Bose fluid ($U < U_{BR}$), E/t vanishes as $\propto (1 - U/U_{BR})^2$, meaning this transition is a continuous type. The difference of the two functions is small for small U/t ($\lesssim 15$), but it becomes conspicuous as U/t approaches Mott critical values ($U/t \gtrsim 20$). Thus, QWF is a considerably improved function in the point of the variation principle.

As we will discuss in detail shortly, QWF also exhibits a superfluid-insulator transition, but its behavior is qualitatively different from that of GWF. In contrast to E of GWF, E of QWF in the insulating regime ($U > U_c$) does not vanish but is proportional to $-t^2/U$ as seen in Fig. 1, which behavior is expected from strong-correlation theories, namely, the density fluctuation does not cease but is re-

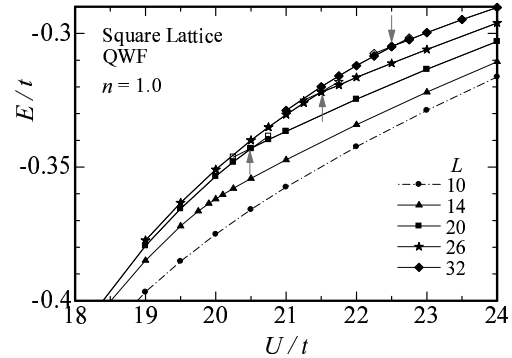


Fig. 2. Magnification of total energy of QWF near Mott transitions arising at $U = U_c$ indicated by arrows. Data for five system sizes are plotted; for $L \geq 20$, double-minimum or cusp behavior is observed at $U = U_c$. Solid symbols denote the energies of the optimized states, and open symbols near U_c metastable states.

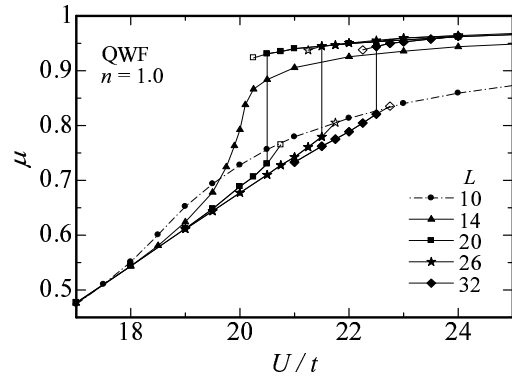


Fig. 3. Behavior of doublon-holon binding parameter near U_c . Data for five system sizes are plotted; for $L \geq 20$, discontinuities are observed at $U = U_c$. Solid and open symbols have the same meaning as in Fig. 2.

stricted to a finite short range. This is the essence of the mechanism of Mott transition owing to the doublon-holon binding. In Fig. 2, we show the magnification of E/t of QWF for $U \sim U_c$. For large L (> 20), we find, near $U = U_c$, double-minimum structure of E/t in the space of variational parameters, meaning this transition is first order, although such structure cannot be confirmed for $L \leq 14$ by our VMC calculations.

The first-order features are more easily found in the variational parameters and in some quantities. In Fig. 3, we plot the optimized doublon-holon binding parameter μ near U_c . For $L \geq 20$, there are clear discontinuities at $U = U_c$; the large values of μ for $U > U_c$ indicate that a doublon and a

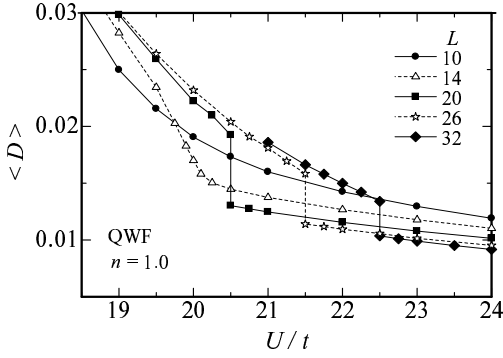


Fig. 4. Behavior of $\langle D \rangle$, which is substantially the doublon density and an order parameter of Mott transitions. Data are shown only for the optimized states.

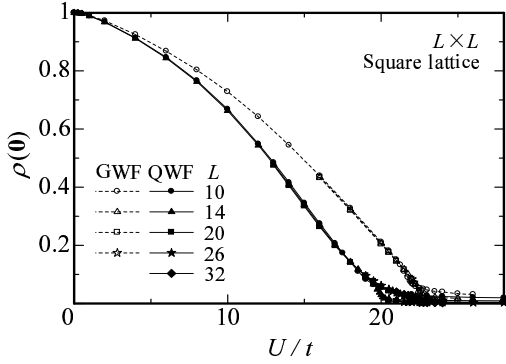


Fig. 5. The occupation rate of the $\mathbf{k} = (0,0)$ level for the two wave functions is depicted as a function of U/t . Data for several system sizes are simultaneously plotted.

holon are tightly bound in nearest-neighbor sites. In Fig. 4, we show the average of D , which is, near U_c , virtually identical with the doublon density, namely, an order parameter of Mott transitions. The discontinuities of this quantity at U_c corroborate a first-order Mott transition.

Finally, let us consider a couple of properties of this Mott transition. In Fig. 5, we show the occupation rate, $\rho(\mathbf{k}) = \langle b_{\mathbf{k}}^\dagger b_{\mathbf{k}} \rangle / N$, of the lowest-energy level, $\mathbf{k} = \mathbf{0} = (0,0)$ versus U/t . Although $\rho(\mathbf{0})$ does not directly indicate the superfluidity, it must be a good index of superfluidity. For the non-interacting case ($U/t = 0$), all the particles fall in the $\mathbf{k} = \mathbf{0}$ level. As the interaction becomes strong, $\rho(\mathbf{0})$ decreases at first gradually and drops discontinuously to the order of $1/N$ at U_c . Thus, the superfluidity vanishes at the transition. In Fig. 5, we plot the chemical potential, $\zeta = \partial E / \partial n$, estimated

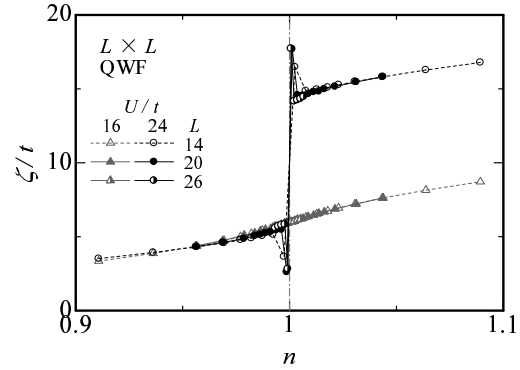


Fig. 6. The Behavior of chemical potential, ζ/t , as a function of particle density near $n = 1$ is shown for two values of U/t , 16 in the superfluid regime and 24 in the insulating regime. Data of three system sizes are simultaneously plotted for each U/t . The singular behavior in ζ at $n = 1$ for $U > U_c$ stems from the singularly low E at $n = 1$ as a function of n .

from finite differences, as a function of n . In the superfluid regime slightly below U_c ($U/t = 16$, gray symbols), ζ is a smooth function of n even at $n = 1$, indicating the state is gapless in density excitation. On the other hand in the insulating regime slightly above U_c ($U/t = 24$, black symbols), ζ has a large discontinuity at $n = 1$; a density excitation gap opens for $U > U_c$ at $n = 1$. The gap behavior is also confirmed by the density correlation function $N(\mathbf{q})$ for small $|\mathbf{q}|$ (not shown).

4. Discussions: In this proceedings, we have found that a wave function with doublon-holon correlation factor, Ψ_Q , qualitatively improve the description of a Mott transition also in a Bose system. Thus, it is probable that the mechanism of Mott transitions for bosons is basically identical to that for fermions. It is urgent to compare theoretical results with experiments particularly of optical lattices. We have left many issues to be discussed, which will be published elsewhere soon. When main calculations here were finished, we became aware that a similar wave function had been studied recently [19].

References

- [1] For instance, M. P. A. Fisher *et al.*, Phys. Rev. B **40**, 546 (1989).

- [2] M. Greiner *et al.* , Nature **415**, 39 (2002).
- [3] D. Jaksch *et al.* , Phys. Rev. B **81**, 3108 (1998).
- [4] W. Krauth, N. Trivedi, Europhys. Lett. **14**, 627 (1991).
- [5] N. Elstner and H. Monien, Phys. Rev. B **59**, 12184 (1999).
- [6] M. Gutzwiller, Phys. Rev. Lett. **10**, 159 (1963).
- [7] W. Krauth, M. Caffarel, J. -P. Bouchaud, Phys. Rev. B **45**, 3137 (1992); D. S. Rokhsar and B. G. Kotliar, Phys. Rev. B **44**, 10328 (1991).
- [8] M. Gutzwiller, Phys. Rev. **137**, A1726 (1965).
- [9] W. Brinkman, T. M. Rice, Phys. Rev. B **2**, 1324 (1970).
- [10] T. A. Kaplan, P. Horsch, P. Fulde, Phys. Rev. Lett. **49**, 889 (1982).
- [11] H. Yokoyama, H. Shiba, J. Phys. Soc. Jpn. **59**, 3669 (1990).
- [12] T. Watanabe, H. Yokoyama, Y. Tanaka, J. Inoue, to be published in this volume.
- [13] H. Yokoyama, Prog. Theor. Phys. **108**, 59 (2002)
- [14] H. Yokoyama, *et al.* , J. Phys. Soc. Jpn. **73**, 1119 (2004); H. Yokoyama, M. Ogata, Y. Tanaka, J. Phys. Soc. Jpn. **75**, 114706 (2006).
- [15] T. Watanabe, *et al.* , J. Phys. Soc. Jpn. **75**, 074707 (2006).
- [16] W. L. McMillan, Phys. Rev. **138**, A442 (1965).
- [17] H. Yokoyama, H. Shiba, J. Phys. Soc. Jpn. **56**, 1490 (1987).
- [18] C. J. Umrigar, K. G. Wilson, J. W. Wilkins, Phys. Rev. Lett. **60**, 1719 (1988).
- [19] M. Capello *et al.* , preprint (cond-mat/0705.2684).